Noncovalent Interactions

DOI: 10.1002/anie.201208021

The Supramolecular Balance for Transition-Metal Complexes: Assessment of Noncovalent Interactions in Phosphoramidite Palladium Complexes**

*Evelyn Hartmann and Ruth M. Gschwind**

For some decades bidentate ligands have prevailed in the field of transition-metal catalysis.[1] The superiority of bidentate ligands over monodentates was explained by the higher conformational rigidity of the ligands and their stronger coordination to the metal.[1b] However, in the last few years monodentate ligands have experienced a revival, and moreover interest in rational ligand design has grown tremendously:[2] Monodentate ligands have been developed which are able to self-assemble in the coordination sphere of the metal center through weak ligand–ligand interactions, such as hydrogen bonding[2d–g] and metal-bridged coordinative bonding.[2h–j] However, the use of weak interligand interactions based on CH–π and π–π interactions for rational ligand design is still very challenging.[2a]

Various experimental and theoretical approaches have been devised to investigate and quantify noncovalent interactions such as hydrogen bonding and π–π stacking and their dependency on solvent properties.[3] The "double-mutant cycles" developed by Fersht et al. have become a powerful thermodynamic tool for the experimental quantification of single noncovalent interactions in proteins and in host–guest model systems.[4] In addition the "molecular torsion balance" developed by Wilcox and co-workers[5] has been applied to quantify CH–π interactions and aromatic interactions in organic molecules.[3a,b] However, no method has been presented to measure the contribution of noncovalent ligand–ligand interactions within transition-metal complexes to date. For guest–host systems binding constants are typically used for the quantification of noncovalent interactions. However, in the case of metal complexes the binding constant reflects not only noncovalent interactions, but primarily metal–ligand binding based on electronic properties such as the σ-donor/π-acceptor properties of the ligands. Therefore, for the measurement of pure ligand–ligand interactions, covalent and noncovalent contributions to the binding constant must be separated. In addition, possible changes in the electronic and electrostatic properties must be considered, that is, changes in the stereoelectronic properties of the metal–ligand bond and of the electrostatic contributions of the dipoles due to reorientation within the ligands upon *cis–trans* isomerization. To the best of our knowledge, it was previously not possible to separate and quantify the contributions of noncovalent interactions (e.g. CH–π and π–π interactions) from stereoelectronic properties and electrostatic interactions in transition-metal complexes.

In this study we present the first method for the quantification of noncovalent ligand–ligand interactions in transition-metal complexes separated from stereoelectronic and electrostatic effects. Based on the formation trends of different phosphoramidite palladium complexes the free energy difference $\Delta\Delta G$ caused by the formation of additional attractive CH–π interactions was determined. Moreover, ^{1}H^{1}H NOESY measurements and ^{1}H chemical shift changes $\Delta\delta$ were used to gain insight into the complex structures and their interaction patterns to establish the reliability of our method.

The basic method presented in this study for measuring noncovalent interactions in transition-metal complexes is not restricted to special ligands or transition metals. Therefore, first the general principle of the supramolecular balance for transition-metal complexes is explained in complexes with the stoichiometry ML_2X_n (M = transition metal, L = chiral ligand, X = achiral ligand; for a schematic illustration see Figure 1):

a) Three chiral ligands, **A**, **A***(enantiomer of **A**), and **B**, are chosen. For each ligand combination **A**/**B** and **A***/**B** an equilibrium between two homocomplexes—ML_2X_n and ML'_2X_n—and one heterocomplex $MLL'X_n$ is formed. In the case of slow-exchange kinetics on the NMR timescale, the free energy $\Delta G°$ of the heterocomplex formation can be determined from the complex integrals according to $\Delta G° = -RT\ln K$ for both equilibria.
b) Provided that no intermolecular interactions exist between the complexes, the selection of two enantiomeric ligands (**A**, **A***) and one enantiopure ligand (**B**) allows for the energetic linkage of the two equilibria. For both ligand combinations homocomplex $M\mathbf{B}_2X_n$ is identical, while homocomplexes $M\mathbf{A}_2X_n$ and $M\mathbf{A}*_2X_n$ are enantiomeric ($\Delta G = 0$). As a result, the free energy difference between the two systems ($\Delta\Delta G = \Delta G°(\mathbf{A}/\mathbf{B}) - \Delta G°(\mathbf{A}*/\mathbf{B})$) directly reflects the energy difference between the two heterocomplexes $M(\mathbf{A})(\mathbf{B})X_n$ and $M(\mathbf{A}*)(\mathbf{B})X_n$.

So far this method can be applied without restrictions on the structure of the ligands or the transition-metal complexes. However, the resulting $\Delta\Delta G$ encompasses energetic differences caused by both stereoelectronic and electrostatic

[*] Prof. Dr. R. M. Gschwind
Institut für Organische Chemie, Universität Regensburg
Universitätsstrasse 31, 93040 Regensburg (Germany)
E-mail: ruth.gschwind@chemie.uni-regensburg.de

[**] We thank Nikola Kastner-Pustet for the processing of the manuscript, Prof. Dr. R. Wolf for helpful discussions, Michael Hammer for assistance with the calculations, and the DFG for financial support.

Supporting information for this article is available on the WWW under http://dx.doi.org/10.1002/anie.201208021.

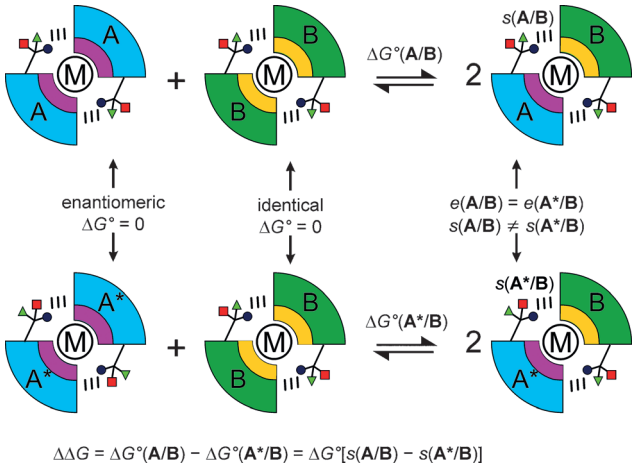

Figure 1. The principle of the supramolecular balance for transition-metal complexes: Two equilibria between homo- and heterocomplexes are linked energetically by combining one enantiopure ligand **B** (green) with two enantiomeric ligands **A** and **A*** (blue). Stereoelectronic and electrostatic properties are represented by pink (e_A, e_{A*}) and yellow (e_B) quadrants, noncovalent interligand interactions (s) by dashed lines. Since identical or enantiomeric homocomplexes are formed, the free energy difference $\Delta\Delta G$ between the two equilibria directly provides the free energy difference between the two heterocomplexes. When the heterocomplexes have identical stereoelectronic and electrostatic properties ($e(\mathbf{A}/\mathbf{B}) = e(\mathbf{A}^*/\mathbf{B})$), the $\Delta\Delta G$ value directly reflects the difference in the noncovalent supramolecular interactions $s(\mathbf{A}/\mathbf{B})$ and $s(\mathbf{A}^*/\mathbf{B})$.

properties e (σ-donor/π-acceptor properties, electrostatic interactions of the dipoles) and supramolecular interactions s within one heterocomplex compared to those in the other. In order to measure pure supramolecular interactions, the electronic contributions must be eliminated. Therefore,

c) ligands and transition-metal complexes are selected which provide identical stereoelectronic and electrostatic effects e but different supramolecular interactions s in the two heterocomplexes ($e(\mathbf{A}/\mathbf{B}) = e(\mathbf{A}^*/\mathbf{B})$; $s(\mathbf{A}/\mathbf{B}) \neq s(\mathbf{A}^*/\mathbf{B})$). As a result, the free energy difference between the two complex equilibria provides exclusively the energetic difference of supramolecular interactions in both heterocomplexes ($\Delta\Delta G = \Delta G°(s(\mathbf{A}/\mathbf{B}) - s(\mathbf{A}^*/\mathbf{B}))$.

By definition two enantiomeric ligands **A** and **A*** possess identical chemical properties in an achiral environment also including stereoelectronic properties such as the σ-donor/π-acceptor character in metal complexes. However, in a chiral environment enantiomers can generally be discriminated by the formation of different interactions. In metal complexes such a chiral environment can be created easily by a simple combination with another chiral ligand, for example, ligand **B**. Thus, supramolecular ligand–ligand interactions in the diastereomeric complexes M(**A**)(**B**)X_n and M(**A***)(**B**)X_n are expected to differ in strength. In order to make use of both of these fundamental properties of enantiomeric ligands for the separation of electronic and supramolecular interactions in metal complexes the electronic properties of **A** and **A*** must stay identical within both diastereomeric complexes M(**A**)(**B**)X_n and M(**A***)(**B**)X_n. That means complexes with clearly defined coordination sites and with identical general structures must be formed. In addition, the orientation of the dipoles has to be retained within M(**A**)(**B**)X_n and M(**A***)(**B**)X_n so that the two complexes have identical electrostatic properties.

Compared to the classical "molecular torsion balance" originally developed by Wilcox,[5] where the consideration of solvation effects[3b,6] is extremely important, our supramolecular balance for transition-metal complexes is quite insensitive to changes in the solvent interactions. Since similar (enantiomeric) ligands are being exchanged and mainly interligand interactions are modified in these equilibria, different solvation properties of the complexes within one solvent are likely to be minimized or even cancelled by virtue of the thermodynamic cycle employed. The application of different solvents can of course affect the absolute strength of the interactions, for example through the dielectric constant.

This method was tested on Pd^{II} complexes using combinations of the well-known phosphoramidite ligands (S_a,R_c,R_c)-**1**,[7] (S_c,S_c)-**2***, and (R_c,R_c)-**2**[8] (see Figure 2b), which find broad application in many asymmetric catalytic

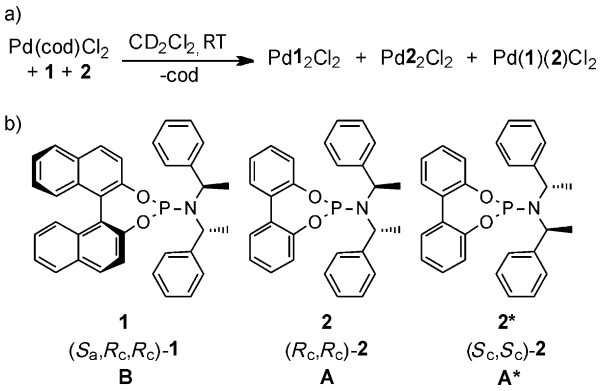

Figure 2. Model system: a) General synthesis of the hetero- and homocomplexes and b) structures of phosphoramidite ligand **1** and the enantiomeric ligands **2** and **2*** used in this study.

reactions.[7–9] Moreover, we could already observe a general affinity of these phosphoramidites to form noncovalent interligand interactions in Cu complexes[10] and in aggregation studies of these ligands and their Cu, Pd, and Ir complexes.[11] In these three ligands, all heteroatoms encompassing the dipoles are located in a very small and structurally rigid inner sphere (O_2PN moieties, see Figure 2b). In addition, all three ligands feature extensive nonpolar outer spheres allowing for the formation of different CH–π and π–π interligand interactions. The chiral centers are located in two amine side chains with high rotational flexibility, which is neither affected by complexation nor by aggregation.[11] Thus, the chiral centers involved in supramolecular interligand interactions are flexibly connected to the inner sphere (see Figure 2b and Figure 1). This allows for different orientations of the chiral parts of **2**, **2***, and **1** without inducing torsional strains on the inner sphere, that is, without affecting the electrostatic and electronic properties of **2** and **2*** in their heterocomplexes with **1**. Provided that identical general complex structures are formed, these structural properties

allow for the formation of transition-metal complexes with a different strength of supramolecular interactions *s*(**2**/**1**) and *s*(**2***/**1**), without affecting the electrostatic properties in the inner spheres of **2**, **2***, and **1**. Thus, the electronic properties *e*(**2**/**1**) and *e*(**2***/**1**) of Pd(**2**)(**1**)Cl_2 and Pd(**2***)(**1**)Cl_2 can be presumed to be identical.

The retention of the general complex structure upon ligand variation was investigated by a small screening of phosphoramidite Pd complexes using four different ligand combinations.[12] After complex synthesis for each ligand combination one heterocomplex PdLL′Cl_2 and two homocomplexes PdL_2Cl_2 and PdL'_2Cl_2 are formed. $^2J_{PP}$ scalar coupling constants between 1150 and 1180 Hz for all heterocomplexes verified the exclusive formation of *trans* complexes, which completely, but slowly convert into *cis* complexes with appropriate $^2J_{PP}$ coupling constants between 95 and 105 Hz.[13] This isomerization to the thermodynamically controlled *cis* complexes[12] is evident in the ^{31}P NMR spectra of the ligand combinations **1**/**2** and **1**/**2*** in Figure 3. In

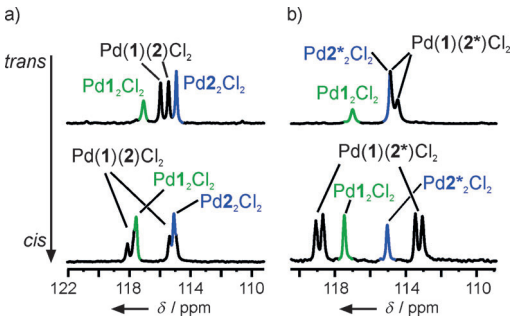

Figure 3. *trans–cis* isomerization of palladium complexes: ^{31}P spectra in CD_2Cl_2 at 300 K of a) Pd(**1**)(**2**)Cl_2 and b) Pd(**1**)(**2***)Cl_2 and corresponding homocomplexes (colored) in exclusive *trans* configuration (top) and after complete conversion into *cis* complexes (bottom).

addition, the interaction pattern is extremely similar within all *cis* complexes Pd(L)(L′)Cl_2 and closely resembles that in the known crystal structure[14] of *cis*-Pd**2***$_2Cl_2$ (see below and the Supporting Information). Therefore, in the following all structural details will be discussed on modifications of this crystal structure (e.g. mirror image and/or extensions of aromatic systems, see Figure 4a).

The extremely high structural similarity of the complexes is best demonstrated by the comparison of the ^{1}H NMR spectra of the homocomplexes *cis*-Pd**1**$_2Cl_2$ and *cis*-Pd**2**$_2Cl_2$ with that of the heterocomplex *cis*-Pd(**1**)(**2**)Cl_2 (Figure 4b). For each homocomplex only one set of signals is detected for both ligands due to their high complex symmetry. The ^{1}H spectrum of the heterocomplex Pd(**1**)(**2**)Cl_2, which contains also both homocomplexes, is almost an addition of the spectra of the corresponding homocomplexes reflecting the high structural similarity. In addition, a change from the homo- to the heterocomplex with retention of the complex structure just exchanges the interacting biaryl groups for both CH and CH_3 in the interligand interactions (see inter(**1**→**2**) and inter(**2**→**1**)). Exactly this structural exchange is reflected by the chemical shift changes observed in the ^{1}H spectra of the

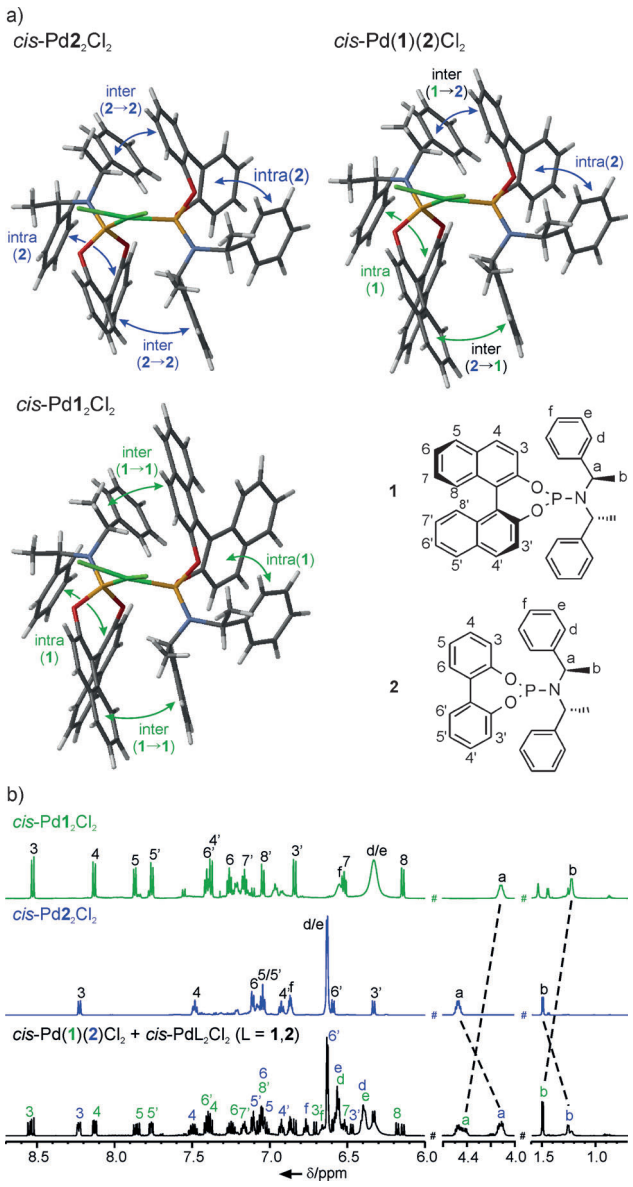

Figure 4. Retention of the complex structure upon ligand variation: a) Inter- and intraligand interactions in *cis*-Pd**2**$_2Cl_2$, *cis*-Pd(**1**)(**2**)Cl_2, and *cis*-Pd**1**$_2Cl_2$ presented on structural models derived from the crystal structure of *cis*-Pd**2***$_2Cl_2$. b) The extreme similarity of the ^{1}H spectra of *cis*-Pd(**1**)(**2**)Cl_2 and the homocomplexes PdL_2Cl_2 (L = **1**, and **2**) indicates the close retention of the general complex structure and of the interaction pattern (600 MHz, CD_2Cl_2, 300 K).

three complexes. There the methine and methyl signals of ligand **1** and **2** in the heterocomplex change places relative to the analogous signals of the corresponding homocomplexes (see signals a and b and dotted lines in Figure 4b; for further details see the Supporting Information).

This close retention of the general complex structure confirms that the electronic properties are not affected by the formation of supramolecular interactions. Therefore, in the next step the free energy contribution of different noncovalent interactions was measured with the double-equilibrium approach shown in Figure 1. Using ligand combinations **1**/**2** and **1**/**2*** the simulations and integrations of the ^{31}P spectra

indeed revealed different homocomplex/heterocomplex ratios (see Figure 3 and the Supporting Information). For the ligand combination **1**/**2*** we observed a ratio of 1.0:0.9:4.5 for the two *cis* homocomplexes and the *cis* heterocomplex, whereas for ligand combination **1**/**2** the homocomplex/heterocomplex ratio approximates the statistical distribution of 1.0:1.1:2.1. According to the formulas described above the free energy difference between the two heterocomplexes *cis*-Pd(**1**)(**2***)Cl_2 and *cis*-Pd(**1**)(**2**)Cl_2 can now be calculated: $\Delta\Delta G = \Delta G(s(\mathbf{2}^*/\mathbf{1}) - s(\mathbf{2}/\mathbf{1})) = -4.82\ \mathrm{kJ\,mol^{-1}}$ (for detailed calculations see the Supporting Information). This value directly describes the stabilization of *cis*-Pd(**1**)(**2***)Cl_2 relative to *cis*-Pd(**1**)(**2**)Cl_2 caused by additional noncovalent supramolecular interactions.

Next $^1H^1H$ NOESY spectra and ^1H chemical shift changes $\Delta\delta$ were used to gain insight into the differences in the noncovalent interactions in the two heterocomplexes. The tube representation of *cis*-Pd(**1**)(**2**)Cl_2 (see Figure 5a) reveals

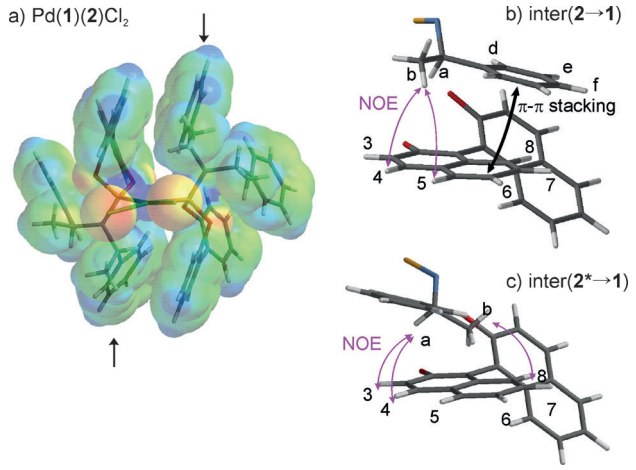

Figure 5. Interligand interactions of *cis*-Pd(**1**)(**2**)Cl_2 versus those of *cis*-Pd(**1**)(**2***)Cl_2: a) Molecular electrostatic potential surfaces of *cis*-Pd(1)(2)Cl_2 (IsoVal: −0.4) calculated at the B3LYP/LACVP level of theory (positive regions blue ($>250\ \mathrm{kJ\,mol^{-1}}$), negative regions red ($<-250\ \mathrm{kJ\,mol^{-1}}$)). A large flat interaction area composed of CH, CH_3, and phenyl groups (see arrows) with the positive charge maximum on CH characterizes the interligand contacts; b,c) details of the interligand interactions inter(**2**→**1**) and inter(**2***→**1**) with experimental NOE contacts show an exchange of the CH_3 and the phenyl group.

that one amine moiety composed of CH, CH_3, and phenyl group forms a large, nearly planar surface which can interact with the biaryl group of the second ligand through CH–π and π–π interactions. Within this contact area a maximum in the molecular electrostatic potential surface indicates that the CH group possesses the highest proton-donating ability (blue in Figure 5a), that is, the greatest stabilizing effect for CH–π interactions.

The main difference between ligands **2** and **2*** lies in the configuration of their amine moiety, which can be seen as a mutual exchange of the CH_3 and the phenyl group. Indeed, $^1H^1H$ NOESY spectra and ^1H chemical shift changes indicate that in the interligand interactions inter(**2**→**1**) the CH_3 group of **2** is exchanged by the phenyl group and vice versa to give inter(**2***→**1**) (see Figure 5b,c and details in the Supporting Information) under retention of the general complex structure. This mutual exchange causes a replacement of two strong π–π interactions in *cis*-Pd(**1**)(**2**)Cl_2 by two strong CH_3–π interactions in *cis*-Pd(**1**)(**2***)Cl_2, and, moreover, a substitution of two weak CH_3–π interactions by two weak π–π interactions. In addition, in inter(**2***→**1**) the CH–π interaction between the CH and the naphthol group is slightly reduced. Of course in a system with such multiple interactions of functional groups, the experimentally determined $\Delta\Delta G$ value cannot be used directly to measure a single functional group interaction. However, the structural investigations show that two phenyl groups are effectively replaced by two CH_3 groups, which in a very rough approximation could be addressed as two additional CH–π interactions. Thus, the calculated $\Delta\Delta G$ value of $-4.8\ \mathrm{kJ\,mol^{-1}}$ is of the right order of magnitude for the structural changes discussed above,[3d,6,15] confirming the applicability of our method. In addition, the formation of large flat interligand interaction areas in both complexes (see Figure 5) suggests that this energy difference should be regarded as a modulation of these extended quasi-planar binding interfaces. Further investigations of structural and formation trends of phosphoramidite palladium complexes show that these modulations in extended quasi-planar CH–π and π–π interaction interfaces might be the refined stereoselection mode that make the phopshoramidites a privileged class of ligands.[12]

In summary, we have presented a method to determine experimentally and quantitatively the contribution of noncovalent interactions within transition-metal complexes. In this general approach the $\Delta\Delta G$ value of two complex equilibria is used as a measure for the deviating noncovalent interactions within the two heterocomplexes. The two equilibria are energetically linked by the combination of one enantiopure ligand with two enantiomeric ligands, leading to identical or enantiomeric homocomplexes. This allows for the separation of supramolecular interactions from stereoelectronic and electrostatic properties provided that the general complex structure is retained. Since this method uses deviating intracomplex interactions within two heterocomplexes, solvation effects of the interacting functional groups are of minor importance. The applicability of this approach was proven with phosphoramidite palladium complexes. The mutual exchange of the CH_3 and the phenyl groups from one ligand to its enantiomer is directly reflected in the NMR data. The experimentally determined $\Delta\Delta G$ value is of the right order of magnitude for the observed changes in the interaction pattern. This example proves for the first time that the catalytically highly important class of phosphoramidite ligands show a pseudo-bidentate character in solution and that modulations in the extended planar CH–π and π–π interaction interfaces cause significant energetic differences.

Received: October 4, 2012
Published online: January 11, 2013

Keywords: intermolecular interactions · NMR spectroscopy · phosphoramidite ligands · transition-metal complexes

[1] a) M. Berthod, G. Mignani, G. Woodward, M. Lemaire, *Chem. Rev.* **2005**, *105*, 1801 – 1836; b) H. B. Kagan, T. P. Dang, *J. Am. Chem. Soc.* **1972**, *94*, 6429 – 6433; c) M. McCarthy, P. J. Guiry, *Tetrahedron* **2001**, *57*, 3809 – 3844.

[2] a) B. Breit, *Angew. Chem.* **2005**, *117*, 6976 – 6986; *Angew. Chem. Int. Ed.* **2005**, *44*, 6816 – 6825; b) S. Carboni, C. Gennari, L. Pignataro, U. Piarulli, *Dalton Trans.* **2011**, *40*, 4355 – 4373; c) M. T. Reetz, *Angew. Chem.* **2008**, *120*, 2592 – 2626; *Angew. Chem. Int. Ed.* **2008**, *47*, 2556 – 2588; d) J. Wieland, B. Breit, *Nat. Chem.* **2010**, *2*, 832 – 837; e) M. de Greef, B. Breit, *Angew. Chem.* **2009**, *121*, 559 – 562; *Angew. Chem. Int. Ed.* **2009**, *48*, 551 – 554; f) Y. Liu, C. A. Sandoval, Y. Yamaguchi, X. Zhang, Z. Wang, K. Kato, K. Ding, *J. Am. Chem. Soc.* **2006**, *128*, 14212 – 14213; g) C. Waloch, J. Wieland, M. Keller, B. Breit, *Angew. Chem.* **2007**, *119*, 3097 – 3099; h) X.-B. Jiang, L. Lefort, P. E. Goudriaan, A. H. M. de Vries, P. W. N. M. van Leeuwen, J. G. de Vries, J. N. H. Reek, *Angew. Chem.* **2006**, *118*, 1245 – 1249; *Angew. Chem. Int. Ed.* **2006**, *45*, 1223 – 1227; i) S. A. Moteki, J. M. Takacs, *Angew. Chem.* **2008**, *120*, 908 – 911; *Angew. Chem. Int. Ed.* **2008**, *47*, 894 – 897; j) J. M. Takacs, D. S. Reddy, S. A. Moteki, D. Wu, H. Palencia, *J. Am. Chem. Soc.* **2004**, *126*, 4494 – 4495.

[3] a) F. Hof, D. M. Scofield, W. B. Schweizer, F. Diederich, *Angew. Chem.* **2004**, *116*, 5166 – 5169; *Angew. Chem. Int. Ed.* **2004**, *43*, 5056 – 5059; b) S. L. Cockroft, C. A. Hunter, *Chem. Commun.* **2006**, 3806 – 3808; c) C. A. Hunter, J. K. M. Sanders, *J. Am. Chem. Soc.* **1990**, *112*, 5525 – 5534; d) S. L. Cockroft, J. Perkins, C. Zonta, H. Adams, S. E. Spey, C. M. R. Low, J. G. Vinter, K. R. Lawson, C. J. Urch, C. A. Hunter, *Org. Biomol. Chem.* **2007**, *5*, 1062 – 1080; e) A. L. Ringer, M. O. Sinnokrot, R. P. Lively, C. D. Sherrill, *Chem. Eur. J.* **2006**, *12*, 3821 – 3828; f) K. E. Riley, M. Piton?ák, P. Jurečka, P. Hobza, *Chem. Rev.* **2010**, *110*, 5023 – 5063; g) E. A. Meyer, R. K. Castellano, F. Diederich, *Angew. Chem.* **2003**, *115*, 1244 – 1287; *Angew. Chem. Int. Ed.* **2003**, *42*, 1210 – 1250.

[4] a) L. Serrano, A. Horovitz, B. Avron, M. Bycroft, A. R. Fersht, *Biochemistry* **1990**, *29*, 9343 – 9352; b) A. Horovitz, A. R. Fersht, *J. Mol. Biol.* **1990**, *214*, 613 – 617; c) P. J. Carter, G. Winter, A. J. Wilkinson, A. R. Fersht, *Cell* **1984**, *38*, 835 – 840; d) S. L. Cockroft, C. A. Hunter, *Chem. Soc. Rev.* **2007**, *36*, 172 – 188.

[5] a) E.-i. Kim, S. Paliwal, C. S. Wilcox, *J. Am. Chem. Soc.* **1998**, *120*, 11192 – 11193; b) S. Paliwal, S. Geib, C. S. Wilcox, *J. Am. Chem. Soc.* **1994**, *116*, 4497 – 4498.

[6] C. A. Hunter, *Angew. Chem.* **2004**, *116*, 5424 – 5439; *Angew. Chem. Int. Ed.* **2004**, *43*, 5310 – 5324.

[7] B. L. Feringa, M. Pineschi, L. A. Arnold, R. Imbos, A. H. M. de Vries, *Angew. Chem.* **1997**, *109*, 2733 – 2736; *Angew. Chem. Int. Ed. Engl.* **1997**, *36*, 2620 – 2623.

[8] A. Alexakis, S. Rosset, J. Allamand, S. March, F. Guillen, C. Benhaim, *Synlett* **2001**, 1375 – 1378.

[9] a) A. Alexakis, D. Polet, *Org. Lett.* **2004**, *6*, 3529 – 3532; b) G. P. Howell, A. J. Minnaard, B. L. Feringa, *Org. Biomol. Chem.* **2006**, *4*, 1278 – 1283; c) R. Imbos, A. J. Minnaard, B. L. Feringa, *Dalton Trans.* **2003**, 2017 – 2023; d) J. F. Jensen, B. Y. Svendsen, T. V. la Cour, H. L. Pedersen, M. Johannsen, *J. Am. Chem. Soc.* **2002**, *124*, 4558 – 4559; e) J. F. Teichert, B. L. Feringa, *Angew. Chem.* **2010**, *122*, 2538 – 2582; *Angew. Chem. Int. Ed.* **2010**, *49*, 2486 – 2528.

[10] K. Schober, E. Hartmann, H. Zhang, R. M. Gschwind, *Angew. Chem.* **2010**, *122*, 2855 – 2859; *Angew. Chem. Int. Ed.* **2010**, *49*, 2794 – 2797.

[11] a) K. Schober, H. Zhang, R. M. Gschwind, *J. Am. Chem. Soc.* **2008**, *130*, 12310 – 12317; b) H. Zhang, R. M. Gschwind, *Chem. Eur. J.* **2007**, *13*, 6691 – 6700.

[12] E. Hartmann, M. Hammer, R. M. Gschwind, *Chem. Eur. J.* **2013**, submitted.

[13] a) A. J. Carty, D. K. Johnson, S. E. Jacobson, *J. Am. Chem. Soc.* **1979**, *101*, 5612 – 5619; b) R. J. Goodfellow, B. F. Taylor, *J. Chem. Soc. Dalton Trans.* **1974**, 1676 – 1684; c) J. G. Verkade, *Coord. Chem. Rev.* **1972**, *9*, 1 – 106; d) J. Mason, *Multinuclear NMR*, Plenum, New York, **1987**; e) F. B. Ogilvie, J. M. Jenkins, J. G. Verkade, *J. Am. Chem. Soc.* **1970**, *92*, 1916 – 1923.

[14] I. S. Mikhel, G. Bernardinelli, A. Alexakis, *Inorg. Chim. Acta* **2006**, *359*, 1826 – 1836.

[15] M. Nishio, *Phys. Chem. Chem. Phys.* **2011**, *13*, 13873 – 13900.

